Design of Hybrid Silicon and Lithium Niobate Active Region for Electro-optical Modulation

Eric G. Martin and Ronald M. Reano
Department of Electrical and Computer Engineering, Electroscience Laboratory
The Ohio State University
Columbus, OH, USA, 43212

Abstract: *We present a design of a hybrid silicon and lithium niobate active region for electro-optical modulation. Modeling and simulation show a DC $V_\pi L$ of 2 V-cm and a 3 dB optical response of 50 GHz.*

Keywords: Integrated optics devices; electro-optics; RF photonics; modulators

Introduction

Lithium niobate has long been a popular platform for electro-optic modulators due largely to the low loss in the telecommunications C-band, large r_{33} electro-optical (Pockels) coefficient (30.8 pm/V), and relatively inexpensive cost of material. Bulk lithium niobate modulators have exhibited 3 dB electro-optical bandwidths of up to 105 GHz [1], making them particularly attractive for RF photonic applications in the millimeter-wave regime. Lithium niobate modulators also exhibit good dynamic range; stemming from the "linear" optical phase change with applied voltage associated with the Pockels effect. However, the half-wave voltage length product, $V_\pi L$, is typically large (~10-20 V-cm) [1–2] because of the small magnitude of the Pockels effect. This weak effect also forces the devices to be long (tens of mm to ~2 cm) for reasonable driving voltages.

In contrast, research in silicon electro-optic modulators in recent years has yielded very efficient devices with $V_\pi L$ below 1 V-cm [3]. Smaller $V_\pi L$ affords shorter devices which when coupled with the silicon platform allow for possible monolithic integration of photonics with electronic components. The efficiency stems from the strong nonlinear index change of the plasma dispersion effect. Unfortunately, these devices are intrinsically limited to a bandwidth of around 60 GHz [4] and operate well under. Additionally, the non-linearity of the plasma dispersion effect negatively impacts the dynamic range of silicon modulators.

Bandwidth and linearity or efficiency and integratability are therefore independently achievable in homogeneous lithium niobate or silicon respectively, but all are not obtainable in either platform independently. In an effort to create modulators that are simultaneously broadband, highly linear, efficient, and integratable researchers have been turning to hybrid integration ([5], [6]) of thin film lithium niobate with "on-insulator" substrates such as lithium niobate-on-insulator (LNOI) and silicon-on-insulator (SOI). Previously our group designed and fabricated a thin-film hybrid lithium niobate ring modulator [7] on a SOI substrate as a proof of concept device. Silicon was used for the optical guiding core with lithium niobate bonded on top via an adhesive. A DC tunability of 5.3 pm/V and modulation bandwidth of 15 GHz were achieved. To achieve a greater modulation bandwidth our group has proposed a Mach-Zehnder traveling-wave type modulator with optimized cross section dimensions using a similar material stack as the previous ring modulator.

Design

Approach: The cross section of the proposed modulator active region is shown in Figure 1. The base substrate for the modulator is a SOI wafer with 3 μm buried oxide height and strip silicon cores providing optical confinement. On top of the silicon waveguides an X-cut lithium niobate cladding is bonded to access the r_{33} electro-optical coefficient for modulation of a TE mode. Rather than attach the lithium niobate cladding via an adhesive, a direct bonding technique will be used instead [8]. It is important to note that this modulator only uses the electro-optic effect and does not utilize the plasma dispersion effect in the silicon waveguide cores. Aluminum electrodes are placed on top of the lithium niobate in a ground signal ground (GSG) co-planar waveguide (CPW) pattern. A CPW is selected because it is electrically broadband and allows for push-pull intensity modulation, which decreases driving voltage by a factor of two when compared to a single drive electrode pair.

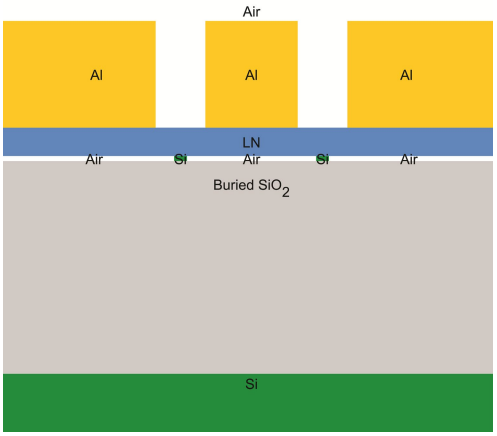

Figure 1. Zoomed cross-section of the proposed modulator active region. The scale is 1:5 horizontal to vertical.

Goals: Several goals were laid out to design the optimal modulator. The most straightforward way to describe

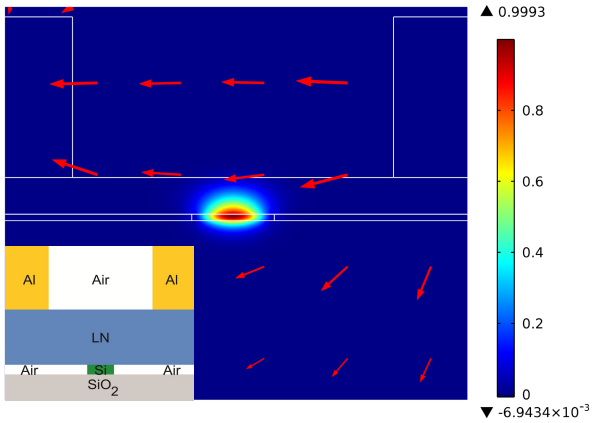

Figure 2. Normalized optical mode intensity with DC electric field lines overlaid.

modulator bandwidth performance is via the optical response which describes the optical modulation depth as a function of frequency. This can also be considered the electrical S_{21} of the modulator relative to DC, neglecting any loss from the photo-detection process. This equation is originally derived in [9] and highlights that bandwidth falls off exponentially with RF losses and degrades as a sinc function with propagation constant mismatch between the RF and optical modes. Thus, our main design goals to maximize bandwidth are to provide a low loss CPW with an RF effective index (n_{RF}) close to that of the single mode optical waveguide (n_{eff}). In addition, a CPW characteristic impedance (Z_0) of 50 Ω is required for compatibility with standard RF systems.

In order to minimize $V_\pi L$, the electro-optic effect must be maximized. The magnitude of the Pockels induced refractive index change is linearly proportional to the applied electric field (RF and DC), so it follows that the electric field should be maximized for a given voltage by the geometry. As previously mentioned, the refractive index change is induced only by the electro-optic effect in the lithium niobate. It is well known that in bulk lithium niobate the induced refractive index change is linearly proportional to the overlap integral between the applied electric field and the optical mode. However, in a bulk modulator the integration is carried out through the entire cross-section, whereas in this modulator active region it is carried out only in the lithium niobate cladding. As a result, it is advantageous to maximize the amount of optical power in the lithium niobate cladding to maximize the electro-optic effect and minimize $V_\pi L$.

Optical: The optical portion of the modulator design served primarily to minimize $V_\pi L$. The following degrees of freedom were allowed to help accomplish this goal:

- Silicon core height and width
- Lithium niobate height
- Gap between the center and ground electrodes

To simulate the optical portion of the modulator, a 2-D COMSOL Multiphysics® eigenvalue mode solver coupled to a static electric field solver is used. First, the mode solver calculates the complex optical mode effective index and electric field distribution. Then, a DC voltage is applied between the electrodes and the field distribution is calculated via the static field solver. The lithium niobate refractive index is programmed to be a function of the applied voltage. By running the optical mode solver twice, the change in optical mode effective index with applied voltage can be determined. From there, $V_\pi L$ is calculated using the method outlined in [10].

RF: The RF portion of the device design was used to maximize the modulator bandwidth. The following degrees of freedom were used to accomplish this goal:

- Center electrode height and width
- Lithium niobate height
- Gap between the center and ground electrodes

It is important to note that the lithium niobate cladding height and the electrode gap couple the optical and RF simulation results. To simulate the RF mode formed by the CPW, another COMSOL Multiphysics® eigenvalue mode solver was used to find the complex RF effective index and characteristic impedance. A design frequency of 40 GHz was selected to match the RF mode effective index to the optical mode effective index and provide a 50 Ω characteristic impedance, after which n_{RF} and Z_0 were calculated as a function of frequency for modulator bandwidth estimation.

Results and Discussion

$V_\pi L$ Considerations: As previously mentioned, to provide a low $V_\pi L$ value the percentage of the optical mode residing the lithium niobate must be maximized. This can be primarily achieved with the silicon core dimensions. Comparing Figure 3 with Figure 4 shows that silicon cores with a narrow height and wide width should be utilized to maximize power in the lithium niobate while maintaining single mode operation.

The lithium niobate cladding height also affects the percentage of the optical power residing within the lithium niobate. As shown in Figure 4 increasing the height of the.

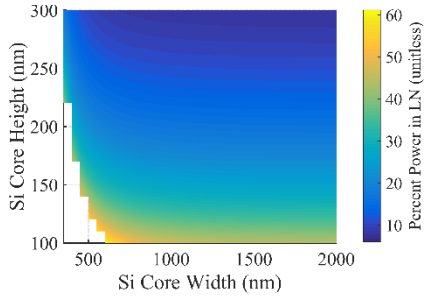

Figure 2. Percentage of optical power in the lithium niobate plotted against silicon core dimensions. The lithium niobate cladding height is 1 μm.

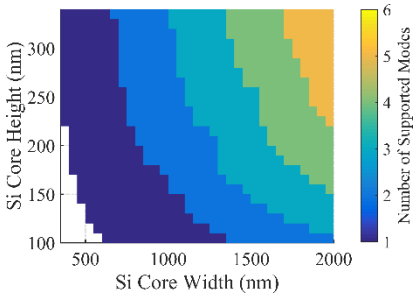

Figure 3. Number of supported optical TE modes plotted against silicon core dimensions. The lithium niobate cladding height is 1 μm.

lithium niobate cladding also increases the power residing within the lithium niobate. However, in doing so the electrodes are moved farther away from the optical mode which decreases the magnitude of the Pockels effect and increases $V_\pi L$. These tradeoffs were used in the determination of the required lithium niobate thickness.

By far the most impactful geometrical parameter in the design on efficiency is the electrode gap. The effect of the electrode gap on $V_\pi L$ is two-fold. Narrowing the electrode gap increases the electric field intensity available to the Pockel's effect. At the same time, the induced metal loss increases as the electrodes become closer to the optical mode. Optical modes that afford more power into the lithium niobate tend to have a larger mode effective area, as indicated by Figure 5, which require a larger electrode gap to keep the metal induced optical loss low. Therefore, the percentage of power in the lithium niobate and the intensity of the static electric field available for the Pockels effect must be balanced through the electrode gap for an optimum $V_\pi L$ value to be realized.

Bandwidth Considerations: The two main impacts on bandwidth were found to be the electrode gap and lithium niobate height. As the electrode gap is narrowed, the RF loss increases as shown in Figure 6, which dominates the optical response. The large lithium niobate RF permittivities of 43 and 28 in the horizontal and vertical directions caused n_{RF} and corresponding refractive index matching to be drastically affected by the lithium niobate height, as shown in Figure 7. The electrode height and width are used to tune both Z_0 and n_{RF} once they are reasonably close to 50 Ω and n_{eff}, determined by the other two parameters.

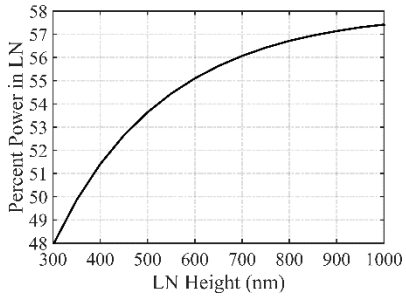

Figure 4. Percentage of the optical power in the lithium niobate plotted against lithium niobate cladding height. The silicon core has a height of 80 nm and width of 1.5 μm.

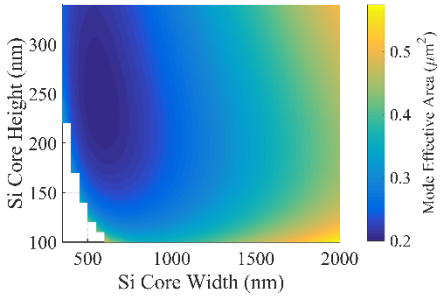

Figure 5. Optical mode effective area plotted against silicon core dimensions. The lithium niobate cladding height is 1 μm.

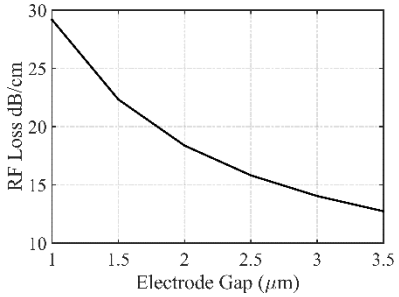

Figure 6. RF losses plotted against the electrode gap. The lithium niobate cladding height, electrode height, and width are 700nm, 2 μm, and 2 μm respectively.

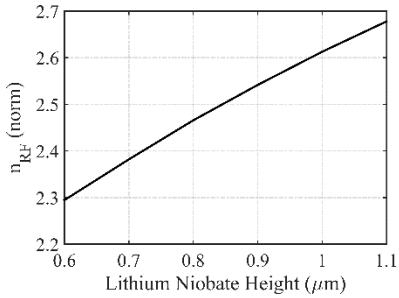

Figure 7. RF losses plotted against the electrode gap. The electrode gap, height, and width are all 2 μm.

Final Design: After considering the impacts on $V_\pi L$ and the modulation bandwidth, it is apparent that a tradeoff between the two exists that is primarily governed by the electrode gap. This tradeoff is non-linear, and our group approached the optimization by holding the electrode gap fixed and letting all other parameters be free. The cross section was

Table 1. Final design parameters.

Lithium Niobate Height (μm)	Si Core Height (μm)	Si Core Width (μm)
0.4	0.07	0.9
Electrode Gap (μm)	Electrode Height (μm)	Center Electrode Width (μm)
3.5	1.5	6.5

then optimized for the lowest $V_\pi L$ while matching n_{RF} to n_{eff} and Z_0 to 50 Ω. This process was carried out iteratively for electrode gaps between 2.5 μm and 5.0 μm with a 500 nm step size. The optimal electrode gap was found to be 3.5 μm. All final design parameters are tabulated in Table 1. The optical mode is displayed in Figure 2. The calculated DC $V_\pi L$ is 2 V-cm for a push-pull dual-drive modulator. The optical mode effective index is 2.07 and the percentage of the power in the lithium niobate is 58%. The induced metal loss is negligible. The optical response is plotted in Figure 8 for an optimized length of 6.5 mm and gives an estimated 3 dB bandwidth of 50 GHz. In addition, $V_\pi L$ remains under 3 V-cm throughout the 50 GHz bandwidth, as shown in Figure 9.

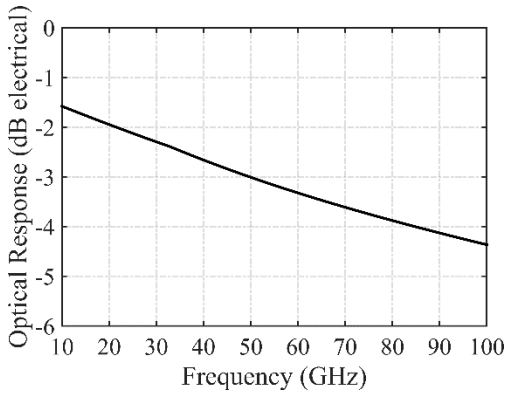

Figure 8. Optical response of the modulator cross-section.

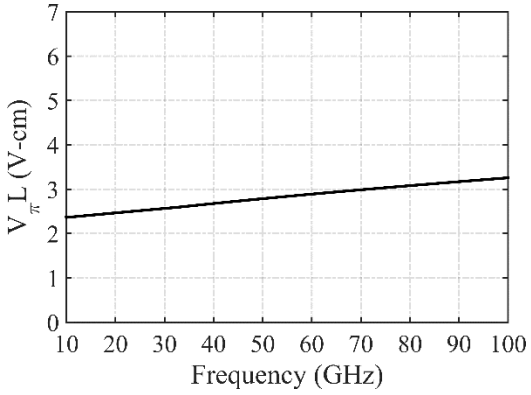

Figure 9. $V_\pi L$ as a function of frequency for a push-pull type modulator cross section.

Conclusion

We have presented the design process and results for a hybrid silicon and lithium niobate active region for electro-optical modulation. The cross section gives an estimated 50 GHz bandwidth with a $V_\pi L$ lower than 3 V-cm throughout the supported frequency band. Future design work includes optical couplers, MMI optical splitters, and an RF launch region to complete the full device layout. Then, a rigorous process flow will be developed to allow for in-house fabrication. This lithium niobate on silicon may be unable to best the bandwidth of homogeneous lithium niobate or the efficiency of silicon, but remains an attractive route towards efficient, densely integrated lower millimeter wave range applications where silicon is not feasible.

Acknowledgement

The authors would like to acknowledge the DAGSI fellowship program as well as Dr. Preetpaul Devgan, Mr. Thomas Dalrymple, and Major Jason Crosby of ARFL/RYDR, WPAFB, Dayton, OH, USA for their funding support of this work.

References

1. K. Noguchi, O. Mitomi, and H. Miyazawa, "Millimeter-wave Ti: $LiNbO_3$ optical modulators," *J. Light. Technol.*, vol. 16, no. 4, p. 615-619, 1998.
2. J. Macario *et al.*, "Full spectrum millimeter-wave modulation," *Opt. Express*, vol. 20, no. 21, p. 23623-23629, Oct. 2012.
3. A. Brimont *et al.*, "Slow light enhanced carrier depletion modulators with 1V drive voltage," 2012, vol. 8431, p. 84310K1–84310K7.
4. F. Y. Gardes, G. T. Reed, N. G. Emerson, and C. E. Png, "A sub-micron depletion-type photonic modulator in silicon on insulator," *Opt. Express*, vol. 24, no. 14, p. 8845–8854, 2005.
5. A. J. Mercante *et al.* "110 GHz CMOS compatible thin film $LiNbO_3$ modulator on silicon," *Opt. Express*, vol. 41, no. 5, p. 15590-15595, July 2016.
6. S. Jin, L. Xu, H. Zhang, and Y. Li, "$LiNbO_3$ Thin-Film Modulators Using Silicon Nitride Surface Ridge Waveguides," *IEEE Photonics Technol. Lett.*, vol. 28, no. 7, pp. 736–739, Apr. 2016.
7. L. Chen, J. Chen, J. Nagy, and R. M. Reano, "Highly linear ring modulator from hybrid silicon and lithium niobate," *Opt. Express*, vol. 23, no. 10, p. 13255-13264, May 2015.
8. P. O. Weigel *et al.*, "Lightwave Circuits in Lithium Niobate through Hybrid Waveguides with Silicon Photonics," *Sci. Rep.*, vol. 6, p. 01-09, Mar. 2016.
9. G. K. Gopalakrishnan *et al.*, "Performance and modeling of broadband $LiNbO_3$ traveling wave optical intensity modulators," *J. Light. Technol.*, vol. 12, no. 10, pp. 1807–1819, Oct. 1994.
10. T. Gorman and S. Haxha, "Design Optimization of Z-Cut Lithium Niobate Electrooptic Modulator with Profiled Metal Electrodes and Waveguides," *J. Light. Technol.*, vol. 25, no. 12, pp. 3722–3729, Dec. 2007.